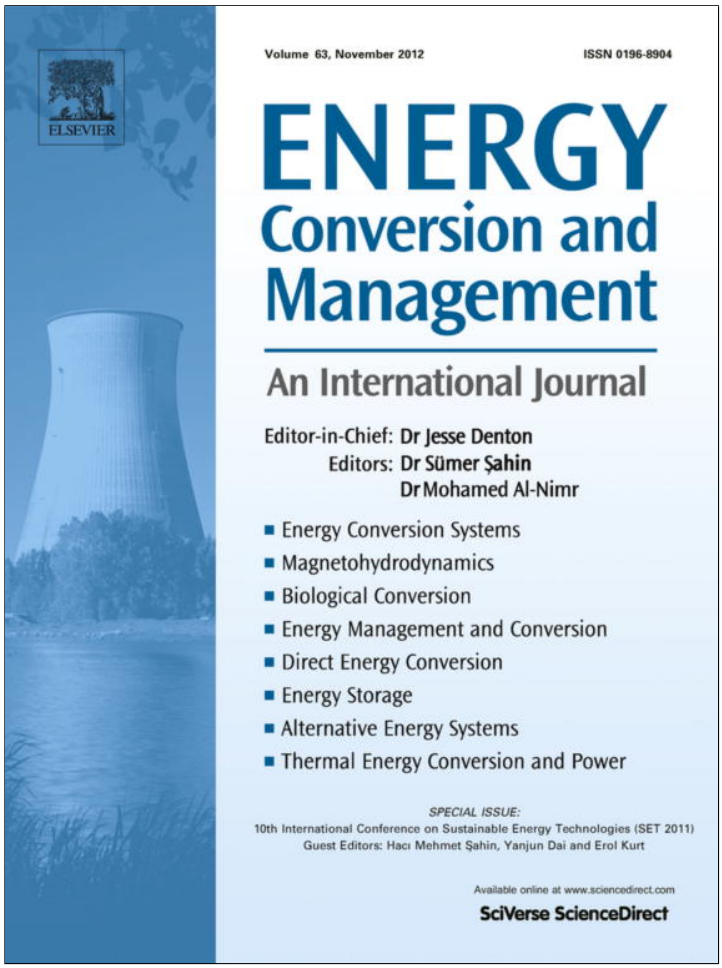

Energy Conversion and Management 63 (2012) 87–94

Contents lists available at SciVerse ScienceDirect

Energy Conversion and Management

journal homepage: www.elsevier.com/locate/enconman

Aerodynamic design of a 300 kW horizontal axis wind turbine for province of Semnan

A. Sedaghat *, M. Mirhosseini

Department of Mechanical Engineering, Isfahan University of Technology, Isfahan 84156-83111, Iran

ARTICLE INFO

Article history:
Available online 12 April 2012

Keywords:
Horizontal axis wind turbine (HAWT)
Aerodynamic design
BEM theory
Chord
Twist

ABSTRACT

In this research, Blade Element Momentum theory (BEM) is used to design a HAWT blade for a 300 kW horizontal axis wind turbine. The airfoil is RISØ-A1-18, produced by RISØ National Laboratory, Denmark. Desirable properties of this airfoil are related to enhancement of aerodynamic and structure interactions. Design parameters considered here are wind tip speed ratio, nominal wind speed and diameter of rotor. The nominal wind speed was obtained from statistical analysis of wind speed data from province of Semnan in Iran. BEM is used for obtaining maximum lift to drag ratio for each elemental constitution of the blade. Obtaining chord and twist distribution at assumed tip speed ratio of blade, the aerodynamic shape of the blade in every part is specified which correspond to maximum accessible power coefficient. The design parameters are trust coefficients, power coefficient, angle of attack, angle of relative wind, drag and lift coefficients, axial and angular induction factors. The blade design distributions are presented versus rotor radius for BEM results. The blade shape then can be modified for ease of manufacturing, structural concerns, and to reduce costs.

1. Introduction

In consideration of the pertinent policies such as geographical position, environmental protection and government's tax allowance, many countries proffered huge funds on technology of wind-power electricity generation and so it developed very fast than compare with technology of thermal power. Utilizing of wind energy has been progressed by more than 50 countries in the whole world considerably [1]. Wind turbines have exhibited their ability to sustain whereas wind energy is a clean, raw material-costless, favorable renewable energy. Wind turbine are classified into two configurations based on their rotational rotor axis with respect to the ground: the older generation, lower-power vertical axis (e.g. Savonius and Darrieus rotor) and the higher power, horizontal-axis at wide commercial deployment (e.g. AWE series 54-900, 52-750, Vestas series v39, and v66, and Nordtank-300).

The potential energy of wind is estimated to be about 6500 MW in Iran [2]. Germany, for example, produced some 4400 MW of electricity from wind; while, Iran with a similar level of available wind power produces approximately 100 MW according to recent news from the ministry of power in Iran [3]. There are abundant wind resources freely available in Northern part of Iran. Manjil, Binalood, and Semnan areas are located in the northern part of the country. There are 21 installed wind turbines in Manjil, 1 with 500 kW, 5 with 550 kW and 15 with 300 kW capacities plus 27 more wind turbines were installed by 1999 in Manjil, Roodbar and Harzevil and recent employment of 28.4 MW in Binalood [3–5]. Semnan province, as shown in Fig. 1, with 5.6% of the whole area of Iran is the sixth big province in the country. Semnan province area is 95,815 km^2. Semnan is located between N34°40′–N37°10′ latitude and E51°59′–E57°4′ longitude [4].

The province of Semnan is bordered from east by the province of Khorasan razavi, from north, Northern Khorasan, Mazandaran and Golestan provinces, from south, Yazd and Esfahan provinces, west, Tehran and Qom provinces. The center of province, Semnan is located at 228 km from Tehran and the distance from international waters of Persian Gulf and Caspian Sea in turn is 1600 and 200 km. This province includes 5 townships, 13 districts, 18 cities and 29 villages. According to the latest statistics in 2001, the population of the province is estimated to be 558,000 that 73.5% were in urban area and 26.5% were rural dwellers [7]. In general, the dominant prevailing wind in the area is blowing from the northwest to the southeast and is called Tooraneh. Also other winds in the province called Shahriari, Kavir and Khorasan winds, blow from west, south and east to west in different seasons of the year, respectively [8,9]. Detailed statistical study of wind at 10 m, 30 m and 40 m height in Semnan province is presented in [4].

2. Aerodynamic of a horizontal axis wind turbine (HAWT)

In the development of modern commercial wind turbines, the size has contiguously increased to the latest multi-MW turbines such as the wind farm shown in Fig. 2. Generally, the two

* Corresponding author.
E-mail address: sedaghat@cc.iut.ac.ir (A. Sedaghat).

0196-8904/$ - see front matter © 2012 Elsevier Ltd. All rights reserved.
http://dx.doi.org/10.1016/j.enconman.2012.01.033

Fig. 1. The location of Semnan province in the map of Iran [6].

Fig. 2. Group of HAWTs in a wind farm in UK [10].

fundamental objectives of the design of a HAWT turbine are to maximize its annual energy production (AEP) and to minimize the cost of energy (COE) produced [11–13]. Recently, focus has been intensified on designing wind turbine rotors for maximum aerodynamic performance [14–22]. According to particularly challenges and difficulties to achieve a good efficiency and thus in obtaining better economical performance, any improvement in the aerodynamic design of wind turbines infers a significant benefit that increase. Aerodynamic efficiency of wind turbines extremely depends on the performance of the rotor blade, the airfoil section, and the design form. The theoretical maximum for the power coefficient, C_p, marked by the Betz limit $C_{p,\max} = 16/27 = 0.593$. Modern horizontal axis wind turbines (HAWTs) work with C_p up to 0.5, nearby the Betz limit [23]. The Blade Element Momentum (BEM) model which is used here is the most common model used in aerodynamic and aero elastic codes for wind turbine performance.

2.1. Wind characteristics in Semnan province

The best way to evaluate the wind resource available at a potential site is by calculating the wind power density. It indicates how much energy is available at the site for conversion to electricity by a wind turbine. The wind power per unit area, P/A or wind power density is related to cube of wind speed U as follow [23]:

$$\frac{P}{A} = \frac{1}{2}\rho U^3 C_p \eta \tag{1}$$

C_p and η are the power coefficient and the electrical–mechanical efficiency, respectively. Based on wind statistics, the annual rated wind speed (the average cubic wind speed) may be used to determine the diameter of the rotor as follow [23]:

$$\frac{\bar{P}}{A} = \frac{1}{2}\int_c^\infty \rho U^3 p(U)dU = \frac{1}{2}\bar{\rho}c^3\Gamma(1+3/k) \approx \frac{1}{2}\bar{\rho}\overline{U^3} \tag{2}$$

where ρ is the air density varied linearly with height (also depends on local air pressure and air speed in actual wind turbine), $\bar{\rho}$ is the average air density at rotor area, Γ is the Gama function, $\overline{U^3}$ is the average cubic wind speed, and $p(U)$ is the Weibull probability density function given by [23]:

$$p(U) = \left(\frac{k}{c}\right)\left(\frac{U}{c}\right)^{k-1}\exp\left[-\left(\frac{U}{c}\right)^k\right] \tag{3}$$

Determination of the Weibull probability density function requires knowledge of two parameters: k, shape factor and c, scale factor also appeared in Eq. (2). Analytical and empirical methods are used to find k and c, such as Justus formulas expressed by [23]:

$$\sigma_u = \sqrt{\frac{\sum_{i=1}^N (U_i - \overline{U})^2}{N-1}} \tag{4}$$

$$k = \left(\frac{\sigma_U}{\overline{U}}\right)^{-1.086}, \quad \frac{c}{\overline{U}} = \frac{k^{2.6674}}{0.184 + 0.816k^{2.73855}} \tag{5}$$

where σ_u and $\overline{U}$ represent the standard deviation and the annual mean wind speed, respectively. Standard deviation also is defined as a function of k [23]:

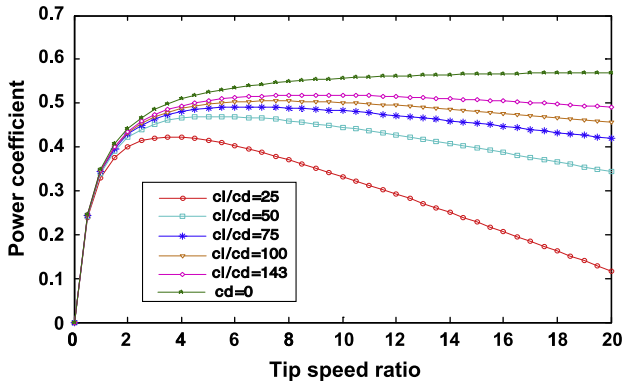

Fig. 3. Power coefficient versus blade tip speed ratio.

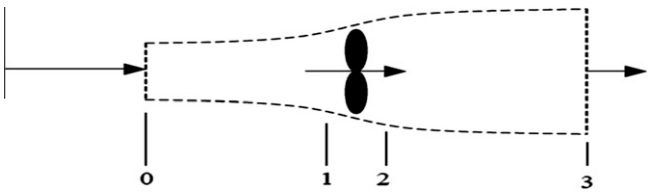

Fig. 4. Actuator disk modelling of a wind turbine in a stream tube.

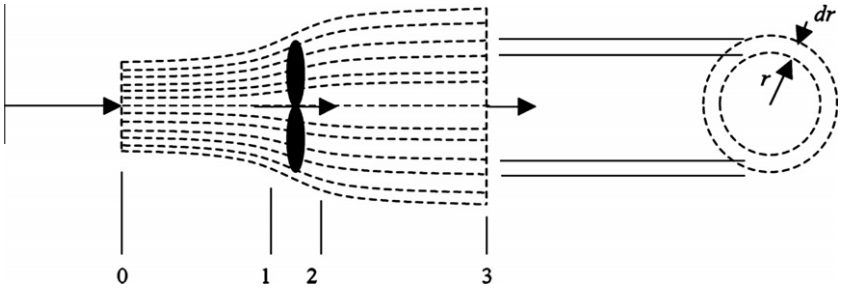

Fig. 5. Annular control volumes for calculating wake rotation.

$$\sigma_U = \overline{U}\sqrt{\left(\frac{\Gamma(1+2/k)}{\Gamma^2(1+1/k)} - 1\right)} \tag{6}$$

For Haddadeh region in province of Semnan in Iran, $k = 1.6$, $c = 6.52$, and the annual mean wind speed and the corresponding rated wind speed is calculated to be 5.85 and 8 at a height of 40 m, respectively [4].

2.2. Rotor specification for HAWTs

The design of the blade requires a great number of design variables parameters to control rotor shape and airfoil characteristics including: the number of blade B, the rotor diameter D, the section airfoil lift to drag ratio that depend on the angle of attack α, and the chord length c, and twist angle θ_t at each section of blade. In commercial HAWTs, it is normally chosen three blades ($B = 3$). If fewer than three blades are selected, there will be a number of structural problems that must be considered in the hub design.

To determine rotor diameter from Eq. (1), the maximum accessible power coefficient, $C_{p,\max}$, is sought. According to the type of application, we need an optimum wind tip speed ratio, defined as the rotational speed of blade tip, $R\Omega$, to the wind speed, U; i.e. $\lambda = R\Omega/U$. For a water pumping windmill, for which greater torque is needed, we use $1 < \lambda < 3$. For electric power generation, we normally use $4 < \lambda < 10$. The machines with higher speeds use less material in the blades and have smaller gearboxes, but require more sophisticated airfoils.

In this work, the maximum accessible power coefficient, $C_{p,\max}$, and the corresponding optimum value of λ_{opt} is calculated from the empirical relation [23]:

$$C_{p,\max} = \left(\frac{16}{27}\right)\lambda\left[\frac{1.32 + \left(\frac{\lambda-8}{20}\right)^2}{B^{2/3}}\right]^{-1} - \frac{(0.57)\lambda^2}{\frac{Cl}{Cd}\left(\lambda + \frac{1}{2B}\right)} \tag{7}$$

Fig. 3 shows a group of C_p–λ curves for a three bladed HAWT from which the optimum value for the tip speed ratio, λ_{opt}, can be obtained for the specified airfoil lift to drag ratio $\frac{Cl}{Cd}$, from the point at which the maximum accessible power coefficient, $C_{p,\max}$, is obtained.

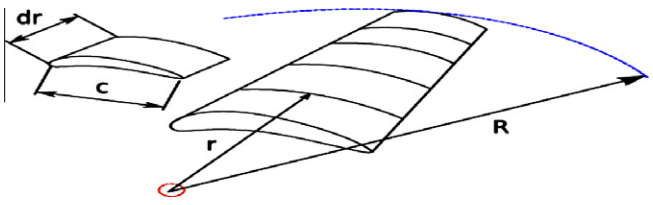

Fig. 6. Annular control volumes for calculating wake rotation.

In order to specify the airfoil type, the maximum lift-to-drag ratio is criterion with other dynamical, roughness sensitivity, and stall behavior of airfoil for the class of wind power considered. Fundamentally, the determination of the rotor size depends on the required energy and blown mean wind speed. As relative wind speed is the resultant of the stream wind speed, blade section speed and rotor induced flow. Lift force is the main force for operating the wind turbine to produce useful power. Airfoils for HAWT are often designed to be used at low attack angle, where the drag coefficient is usually much lower than the lift coefficient. Especially, at blade

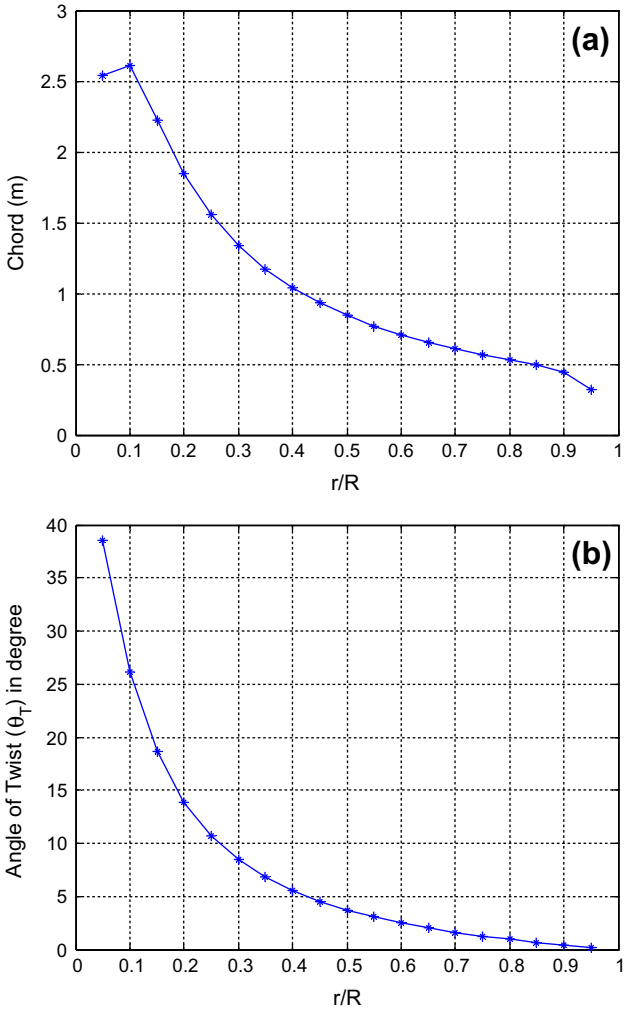

Fig. 7. (a) Chord length distribution and (b) twist angle distribution.

tip airfoils with high lift to drag ratio, low roughness sensitivity, low noise character should be selected to insure the nearest optimum aerodynamic performance. Griffiths [24] showed that the output power is greatly affected by the airfoil lift-to-drag ratio. A general aviation airfoil shape is NACA series, and dedicated airfoil shapes used in modern wind turbines are: S8 series developed by National Renewable Energy Laboratory (NREL) in USA, FFA-W series developed by FOI in Sweden, RISØ-A1 series developed by RISØ in Denmark, DU series developed by Delft University of Technology in Netherlands. It has been found in some applications that more than one airfoil shape can be used for the wind turbine blade design, but there will be bending between these airfoils which may add to uncertainties in the design process.

In this project, the RISØ type airfoils are used [25]. In this class of airfoils, the different families of modern airfoils applied in wind turbines, are verified that with regarding verification of criteria relate to design of wind turbines, the airfoils RISØ-A1-18, FFA-W3-301, FFA-W3-241, DU93-W-210, were proper choices from which RISØ-A1-18 is selected for the 300 kW HAWT in this study [25]. The experimental results of RISØ-A1 are related to open test part of VELUX wind tunnel measurements with 1% turbulence. Details of these tests and measurement instruments are given in [26]. Also the tests were carried out in the Reynolds number equal to 1.6×10^6. A generalized analysis on manufacturing, industrialization, and costs shows that the obtained chord length and twist angle from the theoretical analysis should be modified [27]. Whereas the chord length and twist angle of the wind turbines design are not linear, one procedure for this goal (e.g. simplification in CNC machining for blade's mold manufacturers) is applying fitted linear relationship on the chord length and twist angle curves separately, yet not considered here.

From the experimental data for the RISØ-A-18 airfoil [25], lift coefficient against angle of attack, i.e. Cl–α, and drag coefficient against angle of attack, i.e. Cd–α, is used and approximated by a linear equation for the lift coefficient and a quadratic equation for the drag coefficient versus the angle of attack. The maximum lift to drag ratio (Cl/Cd) is calculated to be $(Cl/Cd)_{\max} = 167$ at the angle of attack of $\alpha = 7^\circ$ for RISØ-A1-18 airfoil. From Fig. 3 for the RISØ-A-18 aerofoil with the maximum lift to drag ratio equals of 167, the optimum tip speed ratio is obtained to be $\lambda_{opt} = 10$ for the corresponding maximum power coefficient of $C_{p,\max} = 0.51$. Assuming a mechanical-electrical efficiency of $\eta = 0.9$ and adopting the rated wind speed of $U = 8\ \frac{m}{s}$ from the statistical analysis of wind data at Semnan province [4], the Rotor diameter is calculated from Eq. (1) to be equals to $D = 54$ m. To obtain an optimum blade shape as a guide, i.e. chord length and twist angle distribution along the blade, the Blade Element Momentum (BEM) theory is employed discussed next [23]. The blade shape then can be modi-

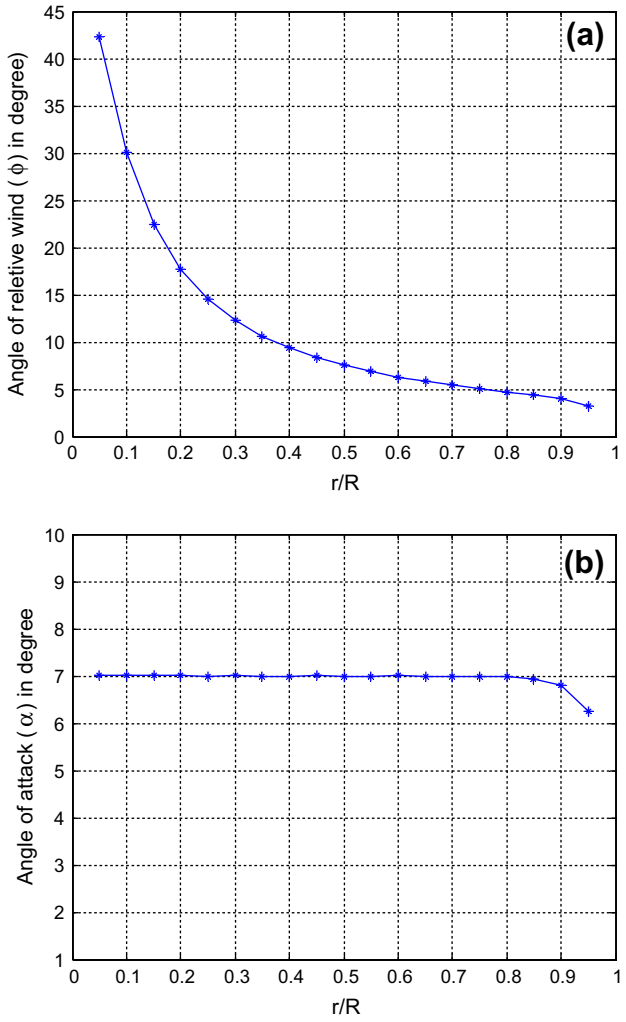

Fig. 8. (a) Angle of relative wind and (b) angle of attack.

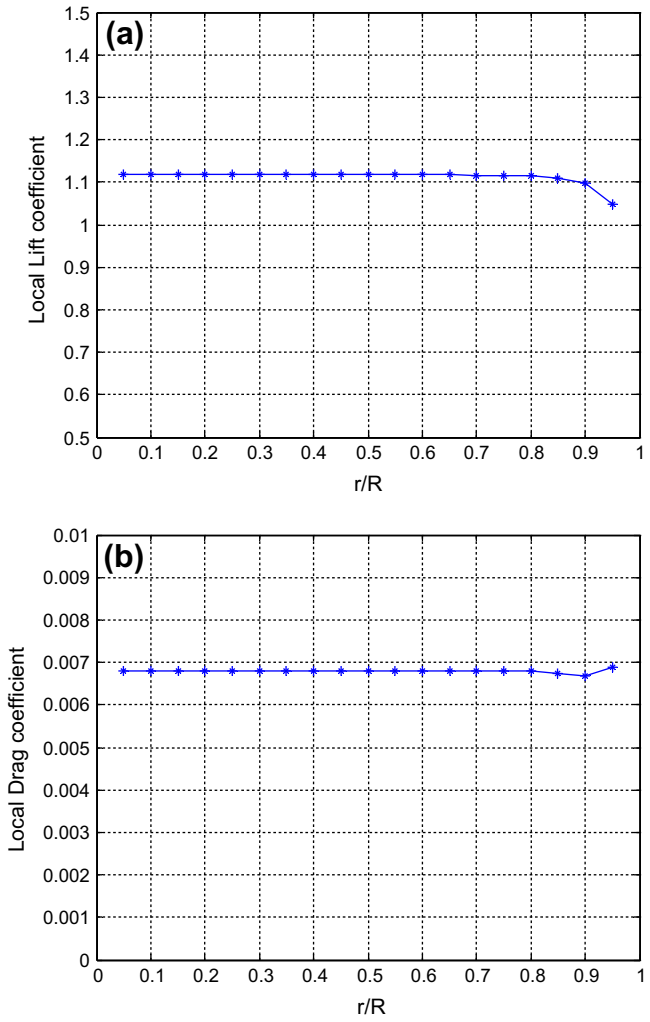

Fig. 9. (a) Lift coefficient and (b) drag coefficient.

fied for ease of manufacturing, structural concerns, and to reduce costs.

2.3. Rotor design using BEM theory

The primitive blade shape is determined using an optimum shape blade considering wake rotating. Ultimate blade shape and its performance are specified with iterative relations and including drag, tip losses and ease of manufacturing. It is also worth emphasizing that with more accurate aerodynamic coefficients at high attack angles, the more accurate design and performance prediction can be obtained. But the aerodynamic coefficients of a rotating airfoil are different from the ones of a linear moving airfoil at stall conditions.

Considering the rotor as an actuator disk which its effects are a sudden drop in pressure and assuming constant speed at the rotor [23], the linear momentum theory is used for air flow through a one dimensional tube as shown in Fig. 4.

From Betz theory, an ideal wind turbine reduces wind speed to two third of the freestream value [23]. Since the wind turbine produces a useful torque for generating power, the conservation of moment of momentum must be satisfied by employing a wake rotation downstream of the wind turbine in some annular control volumes as shown in Fig. 5.

In actuator disk theory, friction drag is ignored which is not realistic. In order to modify this shortcoming [23], blade element theory is considered to incorporate the effects of drag force exerted on each elemental constitution of blade as shown in Fig. 6.

Adopting the procedure discussed in Manwell [23], one may calculate the power coefficient through an iterative method to the following form:

$$C_p = 8/\lambda^2 \int_{\lambda_h}^{\lambda} F\lambda_r^3 \acute{a}(1-a)[1-(Cd/Cl)\cot\theta]d\lambda_r \tag{8}$$

F is tip loss correction factor, a is axial induction factor, $\acute{a}$ is angular induction factor, $\lambda_r = r\Omega/U$ is the local speed ratio for an element of blade at radial distance of r. The element dimension is c as the local chord length and dr as the width of element. The drag to lift ratio (Cd/Cl) corresponds to the local airfoil section.

2.4. Rotor control for HAWTs

In high wind speeds, it is noteworthy to be able to control and limit the rotational mechanical power. The power limitation may be done either by stall control, pitch control or active stall control. Pitch control system in wind turbines have become the more applicable type of installed wind turbines in recent years. For low wind speeds, the speed controller can continuously adjust the speed of

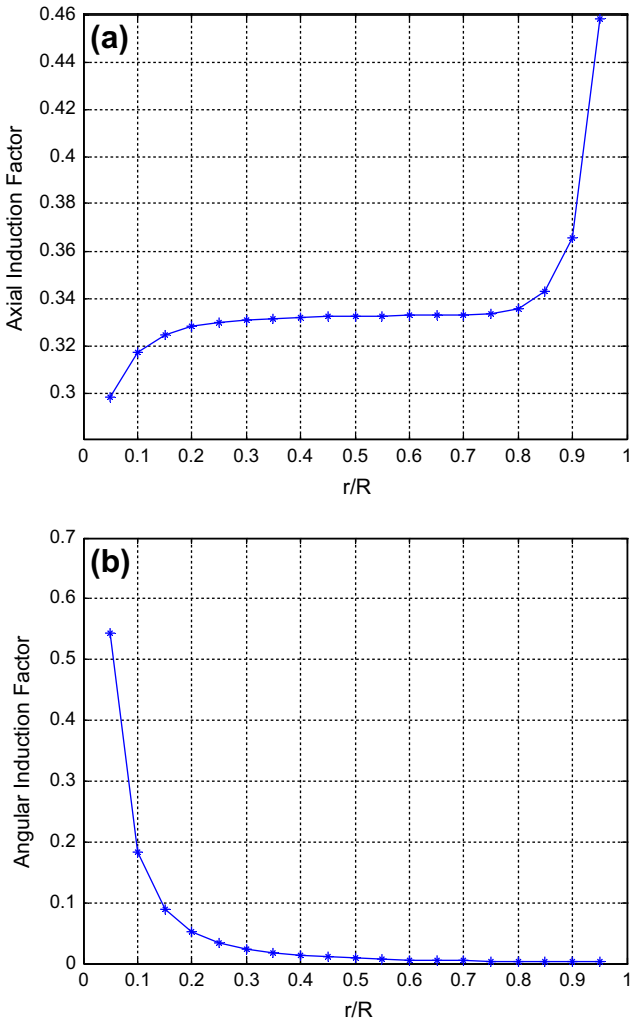

Fig. 10. (a). Axial induction factor and (b) angular induction factor.

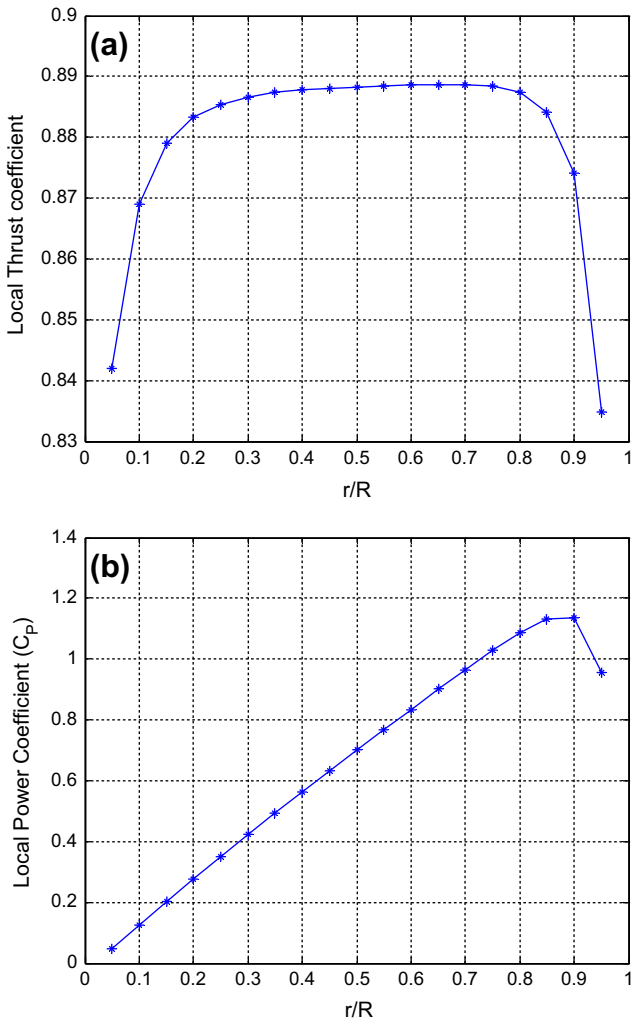

Fig. 11. (a) Trust coefficient and (b) local power coefficient.

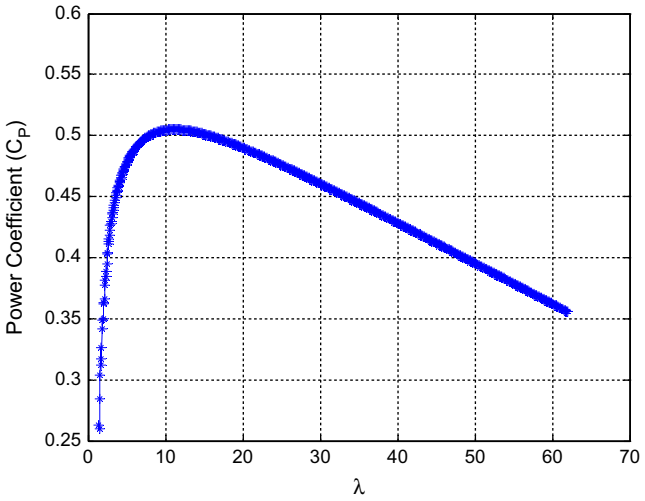

Fig. 12. Power coefficient versus λ.

the rotor to maintain the tip speed ratio constant to produce the maximum power coefficient, and to improve the efficiency of the turbine. For higher wind speeds however pitch angle regulation is required to keep the rotational speed constant. Small changes in pitch angle can reduce considerably the power output. Therefore, the purpose of the pitch angle control may be expressed as [28,29]:

1. Optimizing the power output of the wind turbine.
2. Regulating input mechanical power to avoid exceeding the design limits. Above rated wind speed, pitch angle control provides an effective way to control the aerodynamic power and loads produced by the rotor.
3. Minimizing vibrations and fatigue loads on the turbine mechanical component. Avoiding a generator from over speed by controlling the input mechanical torque, a pitching system has the advantage of actively controlling the input mechanical torque. Although the acceleration of the generator has been limited by the pitch control, the speed of the generator may rise again after the controls have been removed.

3. Results and discussion

Fig. 7a shows that chord length distribution from the BEM analysis. The maximum chord length calculated to be 2.6 m at nearly 10% of blade length from the blade root to the value of nearly 0.3 m at tip. From the practical point of view, higher chord length near the root contribute less to the power gained from wind turbine and therefore it can be modified to reduce material weights and costs and also provide ease of manufacturing [30–33]. Fig. 7b shows the twist angle distribution across the blade length varying from 38° in root to nearly 0° near tip of blade. The twist angle variation along the rotor blade maintains the optimum sectional angle of attack for producing the maximum lift to drag ratio at each section.

In Fig. 8a, the angle of relative wind is varying from 43° in root to 3° at tip producing the much desirable angle of attack value of 7° as shown in Fig. 8b. The angle of attack, α, is constant for the full length of the blade except from 90% of the blade length near to tip that rapidly decreases to values of 6.2° due to tip losses. Tip losses are due to tip vortexes generated at the tip of blades. The undesirable effects of tip losses may be reduced by incorporating new technologies developed in aviation industry [34] such as wingtips implemented in fixed wing aircrafts or reshaping tip blades in aircraft propellers.

Fig. 9a demonstrates that for any angle of attack, *Cl* is almost constant to the value of 1.11 except at the tip which it drops to the value of 1.05. Drag coefficient distribution is shown in Fig. 9b which exhibit a constant value of 0.0069 everywhere. This provides a lift to drag ratio of 161 nearly for 90% of the length of blade a very desirable value for wind turbine blades. For large HAWT blades, the effects of three dimensionality of flow field over blades may be used to include lift losses due to effects of downwash. Downwash effects in non-rotary fixed wings [13] causes a reduction in effective angle of attack and therefore a reduction in lift coefficient.

Fig. 10a shows that the axial induction factor is about 1/3 on most of the blade length ($0.2 < r/R < 0.8$) which increases to a value about 0.46 near tip of the nonlinear blade. However, the angular induction factor attains high values near the root (0.55) which reduces considerably within 10% away from the root of blade as shown in Fig. 10b. This suggest a room for improving aerodynamic characteristics near both the root and the tip of blade using more

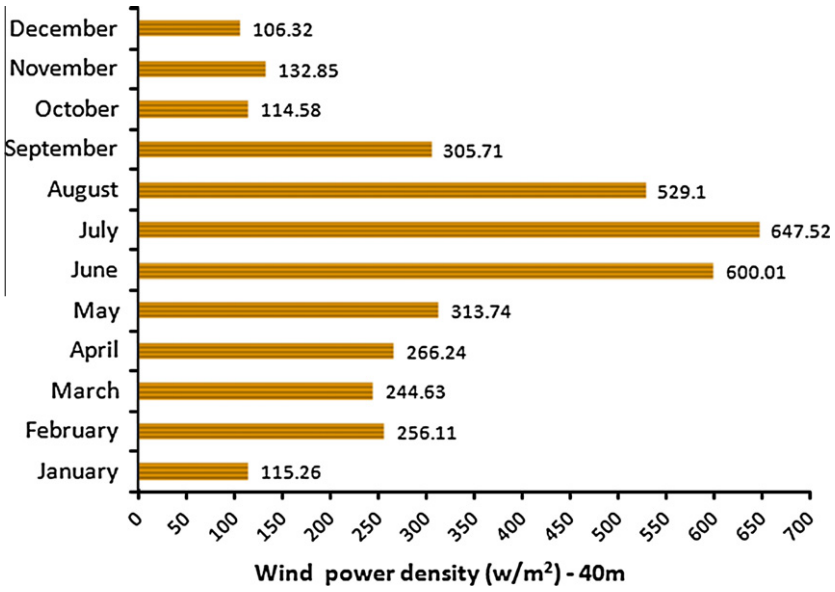

Fig. 13. Monthly power density of Haddadeh at 40 m.

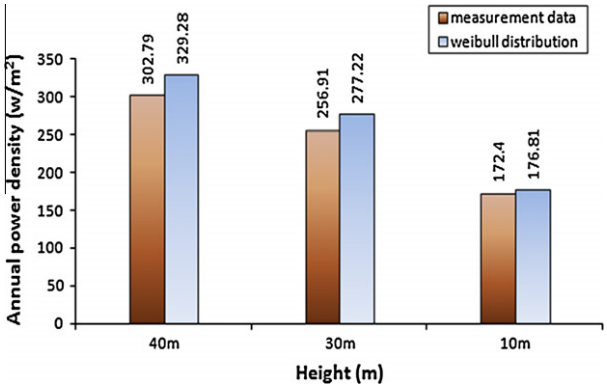

Fig. 14. Annual power density in Haddadeh at 10 m, 30 m and 40 m.

comprehensive methods such as experimental measurements [33] and/or computational fluid dynamics (CFD) techniques [35].

Fig. 11a shows the local thrust coefficient, C_t, which is almost equals to the constant value of nearly 0.88 which gradually decreases to about 0.84 near in both the root and the tip of blade. Fig. 11b shows the power coefficient for the rotor blade which possess its maximum ($C_p = 1.1$) near tip at 90% of the blade length. The variation of power coefficient across the rotor blade is nearly a linear function except a small margin near the tip of blade. An optimum power distribution along the blade may concern with reducing blade's loads towards the tip of blade. This accomplish in some designs by using variable airfoil sections from root to tip of blade to reduce the maximum lift coefficient Cl_{max} at sections near the tip of blade [31].

In Fig. 12, the characteristic performance of the designed blade in terms of the power coefficient C_p against tip speed ratios λ is shown. It is observed that C_p increases to its maximum (0.51) with λ up to its optimum value of 10, and then it decreases at higher tip speed ratio values.

Thus, the predicted aerodynamic characteristics of the designed 300 kW HAWT is achieved according to the initial achievable optimum value of $C_{pmax} = 0.51$ at $\lambda = 10$. The monthly power density of wind at Haddadeh calculated from annual wind data [7] is presented in Fig. 13. The available 10 minutely measured wind data at the heights of 10 m, 30 m, and 40 m were provided by the Iranian renewable energy organisation (SUNA) [36] for the period of 12 months.

Fig. 14 also compares the results from the measured wind data by the Iranian renewable energy organisation (SUNA) [36] and our Weibull distribution which shows power density at height of 40 m is relatively good around 300 W/m^2 for the class of wind turbine designed here.

4. Conclusion

There are abundant high quality wind resources available in Iran; however, the growth of wind turbine industry has been very slow in Iran. This work attempts to address some issues and to preliminary design a site specific 300 kW wind turbine based on manufacturing and economical capabilities and also power demands in the province of Semnan. The positive attitudes in power organization in Iran for moving towards clean and renewable energies have encouraged this type of research in several universities and private organizations in Iran. This as yet requires incentives from European and other developed countries to support research in renewable energies in developing countries both economically and technologically to assist moving faster towards the world of carbon free. To withstand against increasing CO_2 emission into our environment and global warming, imminent international efforts and collaborations are required to further develop and enhance use of wind energy and other renewable resources.

References

[1] Mostafaeipour A. Productivity and development issues of global wind turbine industry. J Renew Sustain Energy Rev 2010;14:1048–58.
[2] News letter from Iranian society of solar energy. A report on the largest wind turbine in Germany with a capacity of 4.5 MW; 2003.
[3] Ministry of power in Iran. <http://news.tavanir.org.ir/press/press_detail.php?id=21481> [accessed November 2011].
[4] Mirhosseini M, Sharifi F, Sedaghat A. Assessing the wind energy potential locations in province of Semnan in Iran. J Renew Sustain Energy Rev 2011;15:449–59.
[5] Kazemi Karegar H, Zahedi A, Ohis V, Taleghani G, Khalaji M. Wind and solar energy development in Iran. North Amir Abad (Tehran/Iran): Centre of Renewable Energy Research and Application; 2006.
[6] Semnan province in Iran. <http://en.wikipedia.org/wiki/Semnan_Province> [accessed November 2011].
[7] Iran chamber society [Internet]. <http://www.iranchamber.com/provinces/25_semnan/25_semnan.php> [cited 12.02.11].
[8] Irano-British quarterly magazine No. 25 [Internet]. <http://ebookbrowse.com/semnan-pdf-d50786496> [cited 18.01.11].
[9] Semnan Meteorological Organization. <http://www.semnanmet.ir>.
[10] Wikipedia [Internet]. <http://en.wikipedia.org/wiki/Wind_farm> [cited 16.11.11].
[11] Wenzhi L, Fuhai ZH, Jianxin W, Changzeng L, 3D modeling methods of aerodynamic shape for large-scale wind turbine blades. In: International conference on information technology and computer science, IEEE conference; 2009. p. 7–10. doi: 10.1109/ITCS.2009.10.
[12] Morgan CA, Garrad AD. The design of optimum rotors for horizontal axis wind turbines, wind energy conversion. In: Milborrow DJ, editor. Proceedings of 1988 tenth BWEA wind energy conference. London: Mechanical Engineering Publications Ltd.; 1988. p. 143–7.
[13] Glauert H. Aerodynamic theory. In: Durand WF, editor. Division L. Airplane propellers, vol. 4, Berlin; 1935. p. 324–30 [chapter XI, reprinted New York: Dover; 1963].
[14] Belessis MA, Stamos DG, Voutsinas SG. Investigation of the capabilities of a genetic optimization algorithm in designing wind turbine rotors. In: Proceedings of European Union wind energy conference and exhibition, Goteborg, Sweden; 1996. p. 124–7.
[15] Selig MS, Coverstone-Carroll VL. Application of a genetic algorithm to wind turbine design. ASME J Energy Resour Technol 1996;118(1):22–8.
[16] Giguere P, Selig MS, Tangler JL. Blade design trade-offs using low-lift airfoils for stall-regulated HAWTs, NREL/CP-500-26091. National Renewable Energy Laboratory, Golden, CO; 1999.
[17] Fuglsang P, Madsen HA. Optimization method for wind turbine rotors. J Wind Eng Ind Aerodyn 1999;80:191–206.
[18] Fuglsang P, Thomsen K. Site-specific design optimization of 1.5–2.0 MW wind turbines. J Solar Energy Eng 2001;123:296–303.
[19] Benini E, Toffolo A. Optimal design of horizontal-axis wind turbines using blade-element theory and evolutionary computation. J Solar Energy Eng 2002;124:357–63.
[20] Tempel JVD, Molenaar DP. Wind turbine structural dynamics. Wind Eng 2002;26(4):211–20.
[21] Jureczko M, Pawlak M, Mezyk A. Optimisation of wind turbine blades. J Mater Process Technol 2005;167:463–71.
[22] Khalfallah MG, Koliub AM. Suggestions for improving wind turbines power curves. Desalination 2007;209:221–9.
[23] Manwell J. Wind energy explained: theory design and application. John Wiley & Sons Inc.; 2002. p. 83–138.
[24] Griffiths RT. The effect of airfoil characteristics on windmill performance. Aeronaut J 1977;81(7):322–6.
[25] Fuglsang P, Sangill O, Hansen P. Design of a 21 m blade with Risø-A1 airfoils for active stall controlled wind turbines. Risø-R-1374(EN), RISØ National Laboratory, Roskilde, December; 2002.
[26] Fuglsang P, Antoniou I, Sørensen NN, Madsen HA. Validation of a wind tunnel testing facility for blade surface pressure measurements. RISØ-R-981(EN), RISØ National Laboratory, Denmark; 1998.
[27] DNV/Risø. Guidelines for design of wind turbines. 2nd ed. Denmark: Jydsk Centraltrykkeri; 2002.
[28] Suryanarayanan S, Dixit A. Control of large wind turbines: review and suggested approach to multivariable design. In: Proceedings of the American control conference, Portland, USA; 2005. p. 686–90.
[29] Burton T, Sharpe D, Jenkins N, Bossanyi E. Wind energy handbook. Chichester (UK): John Wiley & Sons Ltd.; 2001.
[30] Dong L, Liao M, Li Y, Song X, Xu K. Study on aerodynamic design of horizontal axis wind turbine generator system. In: International conference on energy and environment technology, IEEE conference; 2009. p. 841–4. doi: 10.1109/ICEET.2009.208.
[31] Xudong W, Shen WZ, Zhu WJ, Sørensen JN, Jin C. Shape optimization of wind turbine blades. Wind Energy 2009;12:781–803.

[32] Johansen J, Madsen HA, Gaunaa M, Bak C. Design of a wind turbine rotor for maximum aerodynamic efficiency. Wind Energy 2009;12:261–73.
[33] Schreck SJ, Robinson MC. Horizontal axis wind turbine blade aerodynamics in experiments and modeling. IEEE Trans Energy Convers 2007;22(1):61–70.
[34] Madsen HA, Rasmussen F. A near wake model for trailing vorticity compared with the blade element momentum theory. Wind Energy 2004;7:325–41.
[35] Madsen HA. A CFD analysis of the actuator disc flow compared with momentum theory results. In: Proceedings of the 10th symposium on aerodynamics of wind turbines, IEA joint action, Edinburgh; 1996. p. 109–24.
[36] Renewable energies organization of Iran. <http://suna.ir/executivewindand-waves-windenergy-en.html>.